2021 UNC Greensboro PDE Conference,
Electronic Journal of Differential Equations, Conference 26 (2022), pp. 123–138.
ISSN: 1072-6691. URL: http://ejde.math.txstate.edu or http://ejde.math.unt.edu

PENALTY PARAMETER AND DUAL-WIND DISCONTINUOUS GALERKIN APPROXIMATION METHODS FOR ELLIPTIC SECOND ORDER PDES

THOMAS LEWIS, AARON RAPP, YI ZHANG

Abstract. This article analyzes the effect of the penalty parameter used in symmetric dual-wind discontinuous Galerkin (DWDG) methods for approximating second order elliptic partial differential equations (PDE). DWDG methods follow from the DG differential calculus framework that defines discrete differential operators used to replace the continuous differential operators when discretizing a PDE. We establish the convergence of the DWDG approximation to a continuous Galerkin approximation as the penalty parameter tends towards infinity. We also test the influence of the regularity of the solution for elliptic second-order PDEs with regards to the relationship between the penalty parameter and the error for the DWDG approximation. Numerical experiments are provided to validate the theoretical results and to investigate the relationship between the penalty parameter and the L^2-error.

1. Introduction

Let $\Omega \subset \mathbb{R}^d$ be a bounded convex polygonal domain, $f \in L^2(\Omega)$, and $g \in H^{1/2}(\partial\Omega)$. We consider the second order elliptic partial differential problem: find $u \in H^2(\Omega)$ such that

$$-\Delta u = f \quad \text{in } \Omega, \tag{1.1a}$$

$$u = g \quad \text{on } \partial\Omega, \tag{1.1b}$$

where $\Delta u = \sum_{i=1}^{d} \frac{\partial^2}{\partial x_i^2} u$. Dual-Wind Discontinuous Galerkin (DWDG) methods have been applied to the second order elliptic PDE (1.1) as well as its Neumann boundary condition counterpart in [14, 10, 11]. The focus of these papers was to establish *a priori* results for the proposed DWDG methods initially analyzed in a discrete H^1-space inspired by the weak form of (1.1): find $u \in H_g^1(\Omega)$ such that

$$(\nabla u, \nabla v)_\Omega = (f, v)_\Omega \quad \forall v \in H_0^1(\Omega), \tag{1.2}$$

where $(v, w)_\Omega = \int_\Omega vw\, dx$. In this paper we will further investigate properties of the DWDG method and the effects of adding a jump stabilization term since one of

2020 *Mathematics Subject Classification.* 65N30, 65N99.
Key words and phrases. Discontinuous Galerkin methods; DWDG methods; penalty parameter; Poisson problem.
©2022 This work is licensed under a CC BY 4.0 license.
Published August 25, 2022.

the key features of DWDG is the fact that it is naturally stable without penalizing jumps.

There are many continuous Galerkin (CG) methods and discontinuous Galerkin (DG) methods that accurately approximate (1.2) with both weak and strong enforcement of the boundary information. For DG methods, a jump penalization stability term scaled by a penalty parameter γ is introduced in the discrete variational formulation to ensure coercivity; such terms are not needed for CG approximations. It was shown in [5, 6, 12] that a continuous Galerkin method is the limit of a DG interior penalty method as the penalty parameter tends towards infinity. Since DWDG methods are more similar to the more general class of flux-based DG methods such as local discontinuous Galerkin (LDG) methods, a goal of this paper will be to show that DWDG methods will also approach the CG approximation as its limit as $\gamma \to \infty$. We also note that DWDG methods allow for natural enforcement of the Dirichlet boundary condition instead of the typical weak or strong approach.

The penalty parameter γ is an artificial parameter that is traditionally introduced into the discrete formulation of a problem to guarantee the stability of the method in a discontinuous space. For interior-penalty methods, the penalty term naturally occurs in the derivation of a discrete Friedrich's inequality (see [2, 4]). For LDG methods, the parameter does not arise as naturally, and it can be eliminated under certain assumptions in the formulation of the problem [9, 13]. For DWDG methods, the inclusion of an LDG-like penalty term was introduced to ensure stability of the methods for non quasi-uniform meshes. Investigation of the stability and convergence of the dual-wind derivatives and the penalty term for second order elliptic PDEs found that the penalty term was not necessary for a shape-regular mesh. If the mesh was quasi-uniform and each triangle did not have more than one edge on the boundary, then the penalty term could be removed by setting $\gamma_e = 0$ for all edges of a mesh e, or it could be negative as long as $\gamma_e > -C_*$ for some constant $C_* > 0$ (see [13, 14, 10]).

The possibility of a non-positive penalty parameter indicates that DWDG methods naturally weight jumps in the discontinuous approximation space without adding jump terms. The discrete derivatives $\nabla^{\pm}_{h,g}$ themselves control the jumps of the approximation eliminating the need for $\gamma_e \neq 0$ for all edges of the mesh e. This allows us to interpret γ as an artificial penalty parameter for the DWDG methods that can be controlled or eliminated.

We refer the reader to [16] which contains a wide range of numerical experiments that first explored the relationship between the penalty parameter γ and the L^2-error for the DWDG approximation. The numerical experiments in [16] showed a strictly increasing relationship between γ and the L^2-error given that the solution was smooth and the approximation was found on a fine mesh. There was no significant impact from the minimal angle of the mesh, or whether the problem had homogeneous or non-homogeneous boundary conditions. The solutions for the numerical experiments in [16] were either in $C^\infty(\Omega)$ or in the test function space V_h^r. A second goal of this paper will be to extend the initial tests in [16] by experimentally studying the effect of the regularity of the solution to (1.2) on the relationship between γ and the L^2-error.

The rest of the paper is organized as follows. Section 2 introduces notation and briefly discusses the discrete DG interior calculus that will be used to formulate the symmetric dual-wind DG methods in Section 3. In Section 4, we will present

analysis that shows the DWDG methods will converge to a CG method as $\gamma \to \infty$. Numerical experiments verifying the DWDG limit result will be presented in Section 5. Further investigations of the relationship between γ and the L^2-error of the DWDG approximation with regards to the regularity of the solution of (1.2) will also be presented in Section 5.

Throughout this article, C will denote a generic positive constant independent of the mesh size and γ. As such, the constant C can take different values at different occurrences.

2. Notation and DG differential calculus

2.1. **Notation.** We will use the standard space and function notation from [1] and [3] in this paper. Let $W^{m,p}(\Omega)$ denote the set of all $L^p(\Omega)$ functions whose distributional derivatives up to order m are in $L^p(\Omega)$ and $W_0^{m,p}(\Omega)$ denote the set of $W^{m,p}(\Omega)$ functions whose traces vanish up to order $m-1$ on $\partial\Omega$. In the special case where $p=2$, we denote this as $H^m := W^{m,2}$ and $H_0^m := W_0^{m,2}$. Bold-face format will be used for the corresponding vector-valued Sobolev spaces $\mathbf{W}^{m,p}(\Omega) := [W^{m,p}(\Omega)]^d, \mathbf{H}^m(\Omega) := [H^m(\Omega)]^d$, etc. We choose to introduce the discrete derivatives for a general dimension $d \geq 1$ that will be used to formulate the numerical methods and establish our analytic results in Section 4. However, the numerical experiments presented in Section 5 will be done with $d=2$.

Let $\mathcal{T}_h$ denote a shape-regular simplicial triangulation of Ω [3, 8]. Let $\mathcal{E}_h^I$ be the set of interior $(d-1)$-dimensional simplices for the triangulation and $\mathcal{E}_h^B$ the set of boundary $(d-1)$-dimensional simplices so that $\mathcal{E}_h := \mathcal{E}_h^I \cup \mathcal{E}_h^B$. We will denote the diameter of the simplex $K \in \mathcal{T}_h$ as h_K, and we set $h := \max_{K\in\mathcal{T}_h} h_K$. Let d_K represent the diameter of the inscribed circle of a triangle K. A mesh $\mathcal{T}_h$ is shape-regular if there is a constant $C > 0$ such that

$$\max_{K\in\mathcal{T}_h} \frac{h_K}{d_K} \leq C.$$

A mesh $\mathcal{T}_h$ is quasi-uniform if there exist a constant $\rho > 0$ such that

$$\rho < h_K/h_{K'} < \rho^{-1} \quad \forall K, K' \in \mathcal{T}_h.$$

We define the piecewise vector spaces with respect to the triangulation

$$W^{m,p}(\mathcal{T}_h) := \prod_{K\in\mathcal{T}_h} W^{m,p}(K), \quad \mathbf{W}^{m,p}(\mathcal{T}_h) := \prod_{K\in\mathcal{T}_h} \mathbf{W}^{m,p}(K), \text{ etc.}$$

with the special cases $\mathcal{V}_h := W^{1,1}(\mathcal{T}_h) \cap C^0(\mathcal{T}_h)$ and $\boldsymbol{\mathcal{V}}_h := [\mathcal{V}_h]^d$. Let

$$(v,w)_{\mathcal{T}_h} := \sum_{K\in\mathcal{T}_h} \int_K vw\,dx$$

be the piecewise L^2 inner product with respect to the triangulation, and let

$$\langle v,w\rangle_{\mathcal{S}_h} := \sum_{e\in\mathcal{S}_h} \int_e vw\,ds$$

be the piecewise L^2 inner product over any subset $\mathcal{S}_h \subseteq \mathcal{E}_h$. To further simplify notation used later in this paper we will use

$$\langle c_e v,w\rangle_{\mathcal{S}_h} := \sum_{e\in\mathcal{S}_h} \int_e c_e vw\,ds$$

where c_e is a constant that depends on the edge $e \in S_h \subseteq \mathcal{E}_h$. We will also use the following notation for the L^2 norm over the triangularization in this paper:

$$\|v\|^2_{L^2(\mathcal{T}_h)} := (v,v)_{\mathcal{T}_h} \quad \text{and} \quad \|v\|^2_{L^2(\mathcal{S}_h)} := \langle v,v\rangle_{\mathcal{S}_h}$$

for $\mathcal{S}_h \subseteq \mathcal{E}_h$. For an integer $r \geq 1$, we define the DG polynomial space V_h^r to be

$$V_h^r := \prod_{K\in\mathcal{T}_h} \mathbb{P}_r(K),$$

where $\mathbb{P}_r(K)$ denotes the space of polynomials with domain K and degree not exceeding r. We will denote the DG polynomial space with zero-trace over $\partial\Omega$ as $V_{h,0}^r = \{v_h \in V_h^r : v_h = 0 \text{ on } \partial\Omega\}$. As with the vector-valued Sobolev spaces, we will define the vector-valued polynomial spaces using bold-face format; $\mathbf{V}_h^r := [V_h^r]^d$ and $\mathbf{V}_{h,0}^r := [V_{h,0}^r]^d$. For other spaces throughout this paper, we will use bold-face notation to indicate the vector-valued space. We note the inclusions $V_h^r \subset \mathcal{V}_h$ and $\mathbf{V}_h^r \subset \boldsymbol{\mathcal{V}}_h$.

Let $K^+, K^- \in \mathcal{T}_h$, and let $e = \partial K^- \cap \partial K^+ \in \mathcal{E}_h^I$. Without loss of generality we will assume the global labeling number of K^+ is larger than that of K^-. Letting $v_\pm := v|_{K^\pm}$, we define the jumps and averages across the $(d-1)$-dimensional simplex e as

$$[\![v]\!]_e := v_+ - v_-, \quad \{v\}_e := \frac{1}{2}\big(v_+ + v_-\big) \quad \forall v \in \mathcal{V}_h.$$

If K^+ contains an edge in $\mathcal{E}_h^B$, then for the boundary $(d-1)$-dimensional simplex $e = \partial K^+ \cap \partial\Omega$, we define $[\![v]\!]_e := v_+$ and $\{v\}_e := v_+$. Set $(n_e^{(1)}, n_e^{(2)}, \dots, n_e^{(d)})^t = \mathbf{n}_e := \mathbf{n}_{K^+}|_e = -\mathbf{n}_{K^-}|_e$ to be the unit normal on $e \in \mathcal{E}_h$. For $i \in \{1,2,\dots,d\}$ and $v \in \mathcal{V}_h$, we define the labeling-dependent upwind trace operator, $\mathcal{Q}_i^+(v)$, and the labeling dependent downwind trace operator, $\mathcal{Q}_i^-(v)$, on $e \in \mathcal{E}_h^I$ in the direction x_i as

$$\mathcal{Q}_i^\pm(v) := \{v\} \pm \frac{1}{2}\operatorname{sgn}(n_e^{(i)})[\![v]\!], \quad \text{where } \operatorname{sgn}(n_e^{(i)}) = \begin{cases} 1 & \text{if } n_e^{(i)} > 0, \\ -1 & \text{if } n_e^{(i)} < 0, \\ 0 & \text{if } n_e^{(i)} = 0, \end{cases}$$

and $\overline{\mathcal{Q}}_i(v) := \frac{1}{2}\big(\mathcal{Q}_i^-(v) + \mathcal{Q}_i^+(v)\big)$. The operators $\mathcal{Q}_i^-(v)$ and $\mathcal{Q}_i^+(v)$ can be regarded as the "backward" and "forward" limit of v in the x_i direction on $e \in \mathcal{E}_h^I$, , respectively. On a boundary simplex $e \in \mathcal{E}_h^b$, we define $\mathcal{Q}_i^\pm(v) = \overline{\mathcal{Q}}_i(v) = v$.

2.2. **Discontinuous Galerkin calculus.** We use the trace operators $\mathcal{Q}_i^-$, $\mathcal{Q}_i^+$, and $\overline{\mathcal{Q}}_i$ to define our DG discrete partials derivative operators $\partial_{h,x_i}^-, \partial_{h,x_i}^+, \overline{\partial}_{h,x_i} : \mathcal{V}_h \to V_r^h$ that will be used to formulate the DWDG method for approximating (1.2).

Definition 2.1. Let $v \in \mathcal{V}_h$, $g \in L^1(\partial\Omega)$, $i \in \{1,2,\dots,d\}$, let ∂_{x_i} be the usual (weak) partial derivative operator in the direction x_i, and let $n^{(i)}$ be the piecewise constant vector-valued function satisfying $n^{(i)}|_e = [n_e]_i$. The discrete partial derivative operators $\partial_{h,x_i}^\pm, \overline{\partial}_{h,x_i} : \mathcal{V}_h \to V_h^r$ are defined by

$$\begin{aligned} \big(\partial_{h,x_i}^\pm v, \varphi_h\big)_{\mathcal{T}_h} &:= \big\langle \mathcal{Q}_i^\pm(v) n^{(i)}, [\![\varphi_h]\!]\big\rangle_{\mathcal{E}_h} - \big(v, \partial_{x_i}\varphi_h\big)_{\mathcal{T}_h} \quad \forall \varphi_h \in V_h^r, \\ \big(\overline{\partial}_{h,x_i} v, \varphi_h\big)_{\mathcal{T}_h} &:= \big\langle \overline{\mathcal{Q}}_i(v) n^{(i)}, [\![\varphi_h]\!]\big\rangle_{\mathcal{E}_h} - \big(v, \partial_{x_i}\varphi_h\big)_{\mathcal{T}_h} \quad \forall \varphi_h \in V_h^r. \end{aligned}$$

The discrete partial derivatives with given boundary data $\partial^{\pm,g}_{h,x_i}, \overline{\partial}^{g}_{h,x_i} : \mathcal{V}_h \to V_h^r$ are defined as

$$\begin{aligned}
\big(\partial^{\pm,g}_{h,x_i} v, \varphi_h\big)_{\mathcal{T}_h} &:= \big(\partial^{\pm}_{h,x_i} v, \varphi_h)_{\mathcal{T}_h} + \langle (g-v)n^{(i)}, \varphi_h\rangle_{\mathcal{E}_h^B} \quad \forall \varphi_h \in V_h^r,\\
\big(\overline{\partial}^{g}_{h,x_i} v, \varphi_h\big)_{\mathcal{T}_h} &:= \big(\overline{\partial}_{h,x_i} v, \varphi_h)_{\mathcal{T}_h} + \langle (g-v)n^{(i)}, \varphi_h\rangle_{\mathcal{E}_h^B} \quad \forall \varphi_h \in V_h^r.
\end{aligned}$$

Remark 2.2. The definition of $\partial^{\pm,g}_{h,x_i}$ and $\overline{\partial}^{g}_{h,x_i}$ is equivalent to setting $\mathcal{Q}_i^{\pm}(v) = g$ and $\overline{\mathcal{Q}_i}(v) = g$ on $\mathcal{E}_h^B$ implying that the trace data g is naturally incorporated into the discrete partial derivative operator.

Definition 2.3. The discrete gradient operators $\nabla_h^{\pm}, \overline{\nabla}_h, \nabla^{\pm}_{h,g}, \overline{\nabla}_{h,g} : \mathcal{V}_h \to \mathbf{V}_h^r$ are defined as

$$\big[\nabla_h^{\pm} v\big]_i := \partial^{\pm}_{h,x_i} v, \quad \big[\overline{\nabla}_h v\big]_i := \overline{\partial}_{h,x_i} v, \quad \big[\nabla^{\pm}_{h,g} v\big]_i := \partial^{\pm,g}_{h,x_i} v, \quad \big[\overline{\nabla}_{h,g} v\big]_i := \overline{\partial}^{g}_{h,x_i} v.$$

The discrete divergence operators $\mathrm{div}_h^{\pm}, \overline{\mathrm{div}}_h : \boldsymbol{\mathcal{V}}_h \to V_h^r$ are defined as

$$\mathrm{div}_h^{\pm}\, \mathbf{v} := \sum_{i=1}^{d} \partial^{\pm}_{h,x_i} [\mathbf{v}]_i, \quad \overline{\mathrm{div}}_h \mathbf{v} = \frac{1}{2}\big(\,\mathrm{div}_h^{+}\, \mathbf{v} + \mathrm{div}_h^{-}\, \mathbf{v}\big).$$

We end this section by listing some properties of the DG discrete derivatives that will be used in the formulation of our proposed methods. From Definition 2.3, we can relate $\nabla^{\pm}_{h,g}$ and $\nabla^{\pm}_{h,0}$ for all $v, w \in \mathcal{V}_h$ by

$$\big(\nabla^{\pm}_{h,g} v, \boldsymbol{\varphi}_h\big)_{\mathcal{T}_h} = \big(\nabla^{\pm}_{h,0} v, \boldsymbol{\varphi}_h\big)_{\mathcal{T}_h} + \langle g, \boldsymbol{\varphi}_h \cdot \mathbf{n}\rangle_{\mathcal{E}_h^B} \quad \forall \boldsymbol{\varphi}_h \in \mathbf{V}_h^r, \tag{2.1}$$

$$\Big(\nabla^{\pm}_{h,g} v - \nabla^{\pm}_{h,g} w, \boldsymbol{\varphi}_h\Big)_{\mathcal{T}_h} = \Big(\nabla^{\pm}_{h,0} (v-w), \boldsymbol{\varphi}_h\Big)_{\mathcal{T}_h} \quad \forall \boldsymbol{\varphi}_h \in \mathbf{V}_h^r. \tag{2.2}$$

The following discrete analog of integration by parts holds ($i = 1, 2, \ldots, d$), see [11],

$$(\partial^{\pm}_{h,x_i} v_h, \varphi_h)_{\mathcal{T}_h} = -(v_h, \partial^{\mp}_{h,x_i} \varphi_h)_{\mathcal{T}_h} + \langle v_h, \varphi_h n^{(i)}\rangle_{\mathcal{E}_h^B} \quad \forall v_h,\, \varphi_h \in V_h^r \tag{2.3}$$

yielding

$$(\nabla_h^{\pm} v_h, \boldsymbol{\varphi}_h)_{\mathcal{T}_h} = -(v_h, \mathrm{div}_h^{\mp}\, \boldsymbol{\varphi}_h)_{\mathcal{T}_h} + \langle v_h, \boldsymbol{\varphi}_h \cdot \mathbf{n}\rangle_{\mathcal{E}_h^B} \quad \forall v_h \in V_h^r,\ \boldsymbol{\varphi}_h \in \mathbf{V}_h^r, \tag{2.4}$$

$$(\nabla^{\pm}_{h,0} v_h, \boldsymbol{\varphi}_h)_{\mathcal{T}_h} = -(v_h, \mathrm{div}_h^{\mp}\, \boldsymbol{\varphi}_h)_{\mathcal{T}_h} \quad \forall v_h \in V_h^r,\ \boldsymbol{\varphi}_h \in \mathbf{V}_h^r. \tag{2.5}$$

An important property of the DG discrete derivatives is that they are the L^2 projections of the derivative of a function v if $v \in H^1(\Omega)$.

Lemma 2.4 ([11]). *For any $v \in H^1(\Omega)$, both $\partial^{\pm}_{h,x_i} v$ and $\overline{\partial}_{h,x_i} v$ are the L^2 projections of $\partial_{x_i} v$ onto V_h^r; that is, $(\partial^{\pm}_{h,x_i} v, w_h)_{\mathcal{T}_h} = (\overline{\partial}_{h,x_i} v, w_h)_{\mathcal{T}_h} = (\partial_{x_i} v, w_h)_{\mathcal{T}_h}$ for all $w_h \in V_h^r$. Moreover, if $v \in H^1(\Omega)$ satisfies $v|_{\partial\Omega} = g$ for some $g \in L^2(\Omega)$, then both $\partial^{\pm,g}_{h,x_i} v$ and $\overline{\partial}^{g}_{h,x_i} v$ are the L^2 projection of $\partial_{x_i} v$ onto V_h^r.*

From the above lemma, it is possible to derive another useful identity for the discrete differential operators.

Lemma 2.5 ([14]). *Let $v \in H^2(\Omega)$ with $v = g$ on the boundary $\partial\Omega$. Then it holds*

$$-(\Delta v, \varphi_h)_{\mathcal{T}_h} = (\overline{\nabla}_{h,g} v, \overline{\nabla}_{h,0} \varphi)_{\mathcal{T}_h} + \langle \big\{\overline{\nabla}_{h,g} v - \nabla v\big\} \cdot \mathbf{n}, [\![\varphi_h]\!]\rangle_{\mathcal{E}_h} \quad \forall \varphi_h \in V_h^r. \tag{2.6}$$

3. Dual-wind discontinuous Galerkin approximation method for Poisson's equation

Recall that the strong form of Poisson's equation (1.1) is: find a function u such that

$$-\Delta u = f \quad \text{in } \Omega,$$
$$u = g \quad \text{on } \partial\Omega.$$

Now we define the discrete Laplacian operator $\Delta_{h,g} : V_h^r \longrightarrow V_h^r$ by

$$\Delta_{h,g} v_h := \frac{\operatorname{div}_h^+ \nabla_{h,g}^- v_h + \operatorname{div}_h^- \nabla_{h,g}^+ v_h}{2} \quad \forall v_h \in V_h^r, \tag{3.1}$$

which involves an up-wind gradient operator and a down-wind gradient operator utilized in a symmetric way. The DWDG method for (1.1) seeks a function $u_h^\gamma \in V_h^r$ such that

$$-\Delta_{h,g} u_h^\gamma + j_{h,g}(u_h^\gamma) = \mathcal{P}_h f, \tag{3.2}$$

where $\mathcal{P}_h f \in V_h^r$ is the L^2 projection of f onto V_h^r defined by $(\mathcal{P}_h f, v_h)_{\mathcal{T}_h} = (f, v_h)_{\mathcal{T}_h}$ for all $v_h \in V_h^r$ and $j_{h,g} : \mathcal{V}_h \longrightarrow V_h^r$ is a jump penalization/stabilization operator defined by

$$(j_{h,g}(v), w_h)_{\mathcal{T}_h} := \gamma \langle h_e^{-1} [\![v]\!], [\![w_h]\!] \rangle_{\mathcal{E}_h} - \gamma \langle h_e^{-1} g, w_h \rangle_{\mathcal{E}_h^B} \quad \forall w_h \in V_h^r. \tag{3.3}$$

Traditionally for DWDG methods, we can let $\gamma = \gamma_e$ be a piecewise constant for each $e \in \mathcal{E}_h$. However, for this paper we will assume that the "penalty" parameter is constant across all edges, including boundary edges. We say "penalty" because we can set $\gamma \leq 0$ and still have an accurate approximation method [10, 14, 15, 16].

Using (2.5) and (2.1), a direct calculation shows that problem (3.2) is equivalent to finding $u_h^\gamma \in V_h^r$ such that

$$B_{h,\gamma}(u_h^\gamma, v_h) = F_{h,\gamma}(v_h) \quad \forall v_h \in V_h^r, \tag{3.4}$$

where

$$\begin{aligned} B_{h,\gamma}(v_h, w_h) := \frac{1}{2}\Big(\big(\nabla_{h,0}^+ v_h, \nabla_{h,0}^+ w_h\big)_{\mathcal{T}_h} + \big(\nabla_{h,0}^- v_h, \nabla_{h,0}^- w_h\big)_{\mathcal{T}_h} \Big) \\ + \gamma \langle h_e^{-1} [\![v_h]\!], [\![w_h]\!] \rangle_{\mathcal{E}_h} \quad \forall v_h, w_h \in V_h^r, \end{aligned} \tag{3.5}$$

$$F_{h,\gamma}(v) := (f, v)_{\mathcal{T}_h} + \gamma \langle h_e^{-1} g, v \rangle_{\mathcal{E}_h^B} - \langle g, \overline{\nabla}_{h,0} v \cdot \mathbf{n} \rangle_{\mathcal{E}_h^B} \quad \forall v \in \mathcal{V}_h. \tag{3.6}$$

We define the associated discrete energy norms by

$$\|v_h\|_h^2 := \frac{1}{2}\Big(\|\nabla_{h,0}^+ v_h\|_{L^2(\Omega)}^2 + \|\nabla_{h,0}^- v_h\|_{L^2(\Omega)}^2 \Big), \tag{3.7}$$

$$|\!|\!| v_h |\!|\!|_{h,\gamma}^2 := B_{h,\gamma}(v_h, v_h) = \|v_h\|_h^2 + \gamma \sum_{e \in \mathcal{E}_h} \big\| h_e^{-1/2} [\![v_h]\!] \big\|_{L^2(e)}^2. \tag{3.8}$$

Note that $|\!|\!| \cdot |\!|\!|_{h,\gamma}$ is a norm on V_h^r whenever $\gamma \geq 0$ and that the bilinear form $B_{h,\gamma}(\cdot,\cdot)$ is stable with respect to $|\!|\!| \cdot |\!|\!|_{h,\gamma}$ [14, 15].

4. DWDG converges to CG

In this section, we prove analytically that the DWDG approximation (3.4) will converge to a continuous Galerkin (CG) approximation as $\gamma \to \infty$. For this section,

we will assume that $\gamma > 0$. Note that this only requires the mesh to be shape-regular. We will also assume that $g = \Pi_h g$ on $\partial\Omega$ where $\Pi_h g$ is the standard nodal interpolation of g into V_h^r. We define the spaces

$$V_h^c = \{v \in C(\overline{\Omega}) : v|_K \in \mathbb{P}_r(K),\ \forall K \in \mathcal{T}_h\},$$
$$V_{h,0}^c = \{v_h \in V_h^c : v_h = 0 \text{ on } \partial\Omega\}.$$

The following lemma is adapted from [12, Lemma 3.1], and it shows an important equivalence of norms that will be used for our main analytical result. Note that we choose $\gamma = 1$ for (3.5) to define the energy norm in our analysis, and to state the following lemma based on the energy norm $|\!|\!| \cdot |\!|\!|_{h,1}$.

Lemma 4.1. *There is a positive constant C independent of h and γ such that*

$$|\!|\!| w_h |\!|\!|^2_{V_h^r/V_h^c} \le C \sum_{e\in\mathcal{E}_h} \|h_e^{-1/2}[\![w_h]\!]\|^2_{L^2(e)} \quad \forall w_h \in V_h^r/V_h^c,$$

where $|\!|\!| \cdot |\!|\!|_{V_h^r/V_h^c}$ denotes the quotient norm

$$|\!|\!| w_h |\!|\!|_{V_h^r/V_h^c} = \inf_{v\in V_h^c} |\!|\!| w_h + v |\!|\!|_{h,1}.$$

Remark 4.2. The argument in the proof of [12, Lemma 3.1] is for an energy norm derived from a flux-based DG method. However, the proof does not invoke any special properties of the energy norm, and it can be generalized to any flux-based DG energy norm defined over the finite dimensional DG space V_h^r. Thus, we omit the proof.

Recalling that we have assumed that $g = \Pi_h g$ on $\partial\Omega$, the CG approximation corresponds to finding $u_h^c \in V_h^c$ with $u_h^c|_{\partial\Omega} = \Pi_h g$ such that

$$B(u_h^c, v_h) = (f, v_h) \quad \forall v_h \in V_{h,0}^c, \tag{4.1}$$

where $B(v_h, w_h) = (\nabla v_h, \nabla w_h)_{\mathcal{T}_h}$. To prove our main result, we first show u_h^γ satisfies a Galerkin orthogonality condition.

Lemma 4.3. *Let u_h^γ be the solution to the DWDG method* (3.4) *and u_h^c be the solution to the CG method* (4.1)*. Then*

$$B_{h,1}(u_h^c - u_h^\gamma, v_h) = 0 \quad \forall v_h \in V_{h,0}^c.$$

Proof. Let u_h^γ be the solution (3.4), u_h^c be the solution to (4.1), and $v_h \in V_{h,0}^r \subset V_h^r$. By (3.5), (3.4), the fact that $[\![v_h]\!] = 0$ for all $e \in \mathcal{E}_h^I$, and the fact that $v_h = 0$ on $\partial\Omega$, we have

$$\begin{aligned}
&B_{h,1}(u_h^c - u_h^\gamma, v_h)\\
&= B_{h,1}(u_h^c, v_h) - B_{h,1}(u_h^\gamma, v_h)\\
&= B_{h,1}(u_h^c, v_h) - B_{h,\gamma}(u_h^\gamma, v_h) + \langle \frac{\gamma-1}{h_e}[\![u_h^\gamma]\!], [\![v_h]\!]\rangle_{\mathcal{E}_h}\\
&= B_{h,1}(u_h^c, v_h) - F_{h,\gamma}(v_h)\\
&= \frac{1}{2}\Big(\big(\nabla^+_{h,0}u_h^c, \nabla^+_{h,0}v_h\big)_{\mathcal{T}_h} + \big(\nabla^-_{h,0}u_h^c, \nabla^-_{h,0}v_h\big)_{\mathcal{T}_h}\Big)\\
&\quad + \langle h_e^{-1}[\![u_h^c]\!], [\![v_h]\!]\rangle_{\mathcal{E}_h} - F_{h,\gamma}(v_h)\\
&= \frac{1}{2}\big(\nabla^+_{h,0}u_h^c, \nabla^+_{h,0}v_h\big)_{\mathcal{T}_h} + \frac{1}{2}\big(\nabla^-_{h,0}u_h^c, \nabla^-_{h,0}v_h\big)_{\mathcal{T}_h} - F_{h,\gamma}(v_h).
\end{aligned} \tag{4.2}$$

By (2.1) and Lemma 2.4, equation (4.2) becomes

$$\begin{aligned}
&B_{h,1}(u_h^c - u_h^\gamma, v_h)\\
&= \frac{1}{2}\big(\nabla_{h,g}^+ u_h^c, \nabla_{h,0}^+ v_h\big)_{\mathcal{T}_h} + \frac{1}{2}\big(\nabla_{h,g}^- u_h^c, \nabla_{h,0}^- v_h\big)_{\mathcal{T}_h} - \langle g, \overline{\nabla}_{h,0} v_h \cdot \mathbf{n}\rangle_{\mathcal{E}_h^B} - F_{h,\gamma}(v_h)\\
&= \frac{1}{2}\big(\nabla u_h^c, \nabla_{h,0}^+ v_h\big)_{\mathcal{T}_h} + \frac{1}{2}\big(\nabla u_h^c, \nabla_{h,0}^- v_h\big)_{\mathcal{T}_h} - \langle g, \overline{\nabla}_{h,0} v_h \cdot \mathbf{n}\rangle_{\mathcal{E}_h^B}\\
&\quad - F_{h,\gamma}(v_h) \qquad (4.3)\\
&= \big(\nabla u_h^c, \overline{\nabla}_{h,0} v_h\big)_{\mathcal{T}_h} - \langle g, \overline{\nabla}_{h,0} v_h \cdot \mathbf{n}\rangle_{\mathcal{E}_h^B} - F_{h,\gamma}(v_h)\\
&= \big(\nabla u_h^c, \nabla v_h\big)_{\mathcal{T}_h} - \langle g, \overline{\nabla}_{h,0} v_h \cdot \mathbf{n}\rangle_{\mathcal{E}_h^B} - F_{h,\gamma}(v_h)\\
&= \big(f, v_h\big)_{\mathcal{T}_h} - \langle g, \overline{\nabla}_{h,0} v_h \cdot \mathbf{n}\rangle_{\mathcal{E}_h^B} - F_{h,\gamma}(v_h)
\end{aligned}$$

Lastly, by applying (3.6) to (4.3), we have

$$\begin{aligned}
&B_{h,1}(u_h^c - u_h^\gamma, v_h)\\
&= \big(f, v_h\big)_{\mathcal{T}_h} - \langle g, \overline{\nabla}_{h,0} v_h \cdot \mathbf{n}\rangle_{\mathcal{E}_h^B} - (f, v_h)_{\mathcal{T}_h} - \gamma\langle h_e^{-1} g, v_h\rangle_{\mathcal{E}_h^B} + \langle g, \overline{\nabla}_{h,0} v_h \cdot \mathbf{n}\rangle_{\mathcal{E}_h^B}\\
&= -\gamma\langle h_e^{-1} g, v_h\rangle_{\mathcal{E}_h^B} = 0.
\end{aligned}$$

□

Now we prove the main result of our paper. In [16], it was shown through numerical experiments that the L^2-error was following a check-mark trend or strictly increasing as the the choice of γ increased. Based on the DWDG bilinear form (3.5), any jumps in the DWDG approximation will introduce more energy into in discrete system for large values of γ. Intuitively, this would encourage the DWDG approximation to minimize any jumps, making it resemble a continuous Galerkin approximation for large enough values of γ. In the next theorem, we will show that the difference of the DWDG approximation (3.4) and the CG approximation (4.1) in a discrete energy norm will be bounded, and the bound will explicitly depend on the choice of γ and h.

Theorem 4.4. *If $u \in H^{r+1}(\Omega)$ for $r \geq 1$ is the solution to (1.1), u_h^γ is the solution to the DWDG method (3.4), and u_h^c is the solution to the CG method (4.1), then*

$$|\!|\!| u_h^c - u_h^\gamma |\!|\!|_{h,1} \leq \frac{Ch^r}{\gamma} \|u\|_{H^{r+1}(\Omega)}.$$

Proof. Let $u \in H^{r+1}(\Omega)$ be the solution to (1.1), let u_h^γ be the solution to (3.4) and u_h^c be the solution to (4.1). By Lemma 4.3 and the boundedness of $|\!|\!|\cdot|\!|\!|_{h,1}$, we have

$$\begin{aligned}
|\!|\!| u_h^c - u_h^\gamma |\!|\!|_{h,1}^2 &= B_{h,1}(u_h^c - u_h^\gamma, u_h^c - u_h^\gamma)\\
&= B_{h,1}(u_h^c - u_h^\gamma, u_h^c - u_h^\gamma + v) \qquad (4.4)\\
&\leq |\!|\!| u_h^c - u_h^\gamma |\!|\!|_{h,1} |\!|\!| u_h^c - u_h^\gamma + v |\!|\!|_{h,1}
\end{aligned}$$

for any $v \in V_{h,0}^c$. Dividing both sides of (4.4) by $|\!|\!| u_h^c - u_h^\gamma |\!|\!|_{h,1}$, we obtain

$$|\!|\!| u_h^c - u_h^\gamma |\!|\!|_{h,1} \leq |\!|\!| u_h^c - u_h^\gamma + v |\!|\!|_{h,1} \qquad (4.5)$$

for all $v \in V_{h,0}^c$. Since this holds for all $v \in V_{h,0}^c$, we have by Lemma 4.1 that

$$\begin{aligned}
\|\!| u_h^c - u_h^\gamma |\!\|_{h,1} &\le \inf_{v \in V_{h,0}^c} \|\!| u_h^c - u_h^\gamma + v |\!\|_{h,1} \\
&= \|\!| u_h^c - u_h^\gamma |\!\|_{V_h^r / V_{h,0}^c} \\
&\le C\Big(\sum_{e \in \mathcal{E}_h} \|h_e^{-1/2} [\![u_h^c - u_h^\gamma]\!]\|_{L^2(e)}^2 \Big)^{1/2}.
\end{aligned} \tag{4.6}$$

By (3.5) we have

$$\begin{aligned}
&\gamma \sum_{e \in \mathcal{E}_h} \|h_e^{-1/2} [\![u_h^c - u_h^\gamma]\!]\|_{L^2(e)}^2 \\
&\le B_{h,\gamma}(u_h^c - u_h^\gamma, u_h^c - u_h^\gamma) \\
&= B_{h,\gamma}(u_h^c - u, u_h^c - u_h^\gamma) + B_{h,\gamma}(u - u_h^\gamma, u_h^c - u_h^\gamma).
\end{aligned} \tag{4.7}$$

Now we consider the first term on the right-hand side of (4.7). Recall our assumption $\Pi_h g = g$, which implies $u_h^c - u \in H_0^1(\Omega)$. By the Cauchy-Schwarz inequality and the fact that $[\![u_h^c - u]\!]_e = 0$ for all $e \in \mathcal{E}_h$, we have

$$\begin{aligned}
B_{h,\gamma}(u_h^c - u, u_h^c - u_h^\gamma) &\le \frac{1}{2} \|\nabla_{h,0}^+ (u_h^c - u)\|_{L^2(\mathcal{T}_h)} \|\nabla_{h,0}^+ (u_h^c - u_h^\gamma)\|_{L^2(\mathcal{T}_h)} \\
&\quad + \frac{1}{2} \|\nabla_{h,0}^- (u_h^c - u)\|_{L^2(\mathcal{T}_h)} \|\nabla_{h,0}^- (u_h^c - u_h^\gamma)\|_{L^2(\mathcal{T}_h)} \\
&\quad + \gamma \sum_{e \in \mathcal{E}_h} \langle h_e^{-1} [\![u_h^c - u]\!], [\![u_h^c - u_h^\gamma]\!] \rangle_{L^2(e)} \\
&= \frac{1}{2} \|\nabla_{h,0}^+ (u_h^c - u)\|_{L^2(\mathcal{T}_h)} \|\nabla_{h,0}^+ (u_h^c - u_h^\gamma)\|_{L^2(\mathcal{T}_h)} \\
&\quad + \frac{1}{2} \|\nabla_{h,0}^- (u_h^c - u)\|_{L^2(\mathcal{T}_h)} \|\nabla_{h,0}^- (u_h^c - u_h^\gamma)\|_{L^2(\mathcal{T}_h)}.
\end{aligned}$$

By Lemma 2.4, (3.8) with our assumption that $\gamma > 0$, and (4.6), we have

$$\begin{aligned}
B_{h,\gamma}(u_h^c - u, u_h^c - u_h^\gamma) &= \frac{1}{2} \|\nabla_{h,0}^+ (u_h^c - u)\|_{L^2(\mathcal{T}_h)} \|\nabla_{h,0}^+ (u_h^c - u_h^\gamma)\|_{L^2(\mathcal{T}_h)} \\
&\quad + \frac{1}{2} \|\nabla_{h,0}^- (u_h^c - u)\|_{L^2(\mathcal{T}_h)} \|\nabla_{h,0}^- (u_h^c - u_h^\gamma)\|_{L^2(\mathcal{T}_h)} \\
&= \frac{1}{2} \|\nabla_{h,0}^+ (u_h^c - u)\|_{L^2(\mathcal{T}_h)} \Big(\|\nabla_{h,0}^+ (u_h^c - u_h^\gamma)\|_{L^2(\mathcal{T}_h)} \\
&\quad + \|\nabla_{h,0}^- (u_h^c - u_h^\gamma)\|_{L^2(\mathcal{T}_h)} \Big) \\
&\le \frac{1}{2} \|u_h^c - u\|_h \left(2 \|u_h^c - u_h^\gamma\|_h\right) \\
&\le \|\!| u_h^c - u |\!\|_{h,1} \|\!| u_h^c - u_h^\gamma |\!\|_{h,1} \\
&\le C \|\!| u_h^c - u |\!\|_{h,1} \Big(\sum_{e \in \mathcal{E}_h} \|h_e^{-1/2} [\![u_h^c - u_h^\gamma]\!]\|_{L^2(e)}^2 \Big)^{1/2}.
\end{aligned} \tag{4.8}$$

We will next consider the second term on the right-hand side of (4.7). By (3.4) and (3.5), we have

$$\begin{aligned}
&B_{h,\gamma}(u-u_h^\gamma, u_h^c-u_h^\gamma)\\
&= B_{h,\gamma}(u, u_h^c-u_h^\gamma) - B_{h,\gamma}(u_h^\gamma, u_h^c-u_h^\gamma)\\
&= B_{h,\gamma}(u, u_h^c-u_h^\gamma) - F_{h,\gamma}(u_h^c-u_h^\gamma)\\
&= \frac{1}{2}\Big(\big(\nabla_{h,0}^+ u, \nabla_{h,0}^+(u_h^c-u_h^\gamma)\big)_{\mathcal{T}_h} + \big(\nabla_{h,0}^- u, \nabla_{h,0}^-(u_h^c-u_h^\gamma)\big)_{\mathcal{T}_h}\Big)\\
&\quad + \gamma\langle h_e^{-1}u, (u_h^c-u_h^\gamma)\rangle_{\mathcal{E}_h^B} - F_{h,\gamma}(u_h^c-u_h^\gamma).
\end{aligned} \tag{4.9}$$

Next, by applying (3.6), (2.1), and Lemma 2.5 to (4.9), we have

$$\begin{aligned}
&B_{h,\gamma}(u-u_h^\gamma, u_h^c-u_h^\gamma)\\
&= \frac{1}{2}\big(\nabla_{h,0}^+ u, \nabla_{h,0}^+(u_h^c-u_h^\gamma)\big)_{\mathcal{T}_h} + \frac{1}{2}\big(\nabla_{h,0}^- u, \nabla_{h,0}^-(u_h^c-u_h^\gamma)\big)_{\mathcal{T}_h}\\
&\quad + \gamma\langle h_e^{-1}u, u_h^c-u_h^\gamma\rangle_{\mathcal{E}_h^B} - (f, u_h^c-u_h^\gamma)_{\mathcal{T}_h} - \gamma\langle h_e^{-1}g, u_h^c-u_h^\gamma\rangle_{\mathcal{E}_h^B}\\
&\quad + \langle g, \overline{\nabla}_{h,0}(u_h^c-u_h^\gamma)\cdot\mathbf{n}\rangle_{\mathcal{E}_h^B}\\
&= \frac{1}{2}\big(\nabla_{h,g}^+ u, \nabla_{h,0}^+(u_h^c-u_h^\gamma)\big)_{\mathcal{T}_h} + \frac{1}{2}\big(\nabla_{h,g}^- u, \nabla_{h,0}^-(u_h^c-u_h^\gamma)\big)_{\mathcal{T}_h} - (f, u_h^c-u_h^\gamma)_{\mathcal{T}_h}\\
&= \big(\overline{\nabla}_{h,g}u, \overline{\nabla}_{h,0}(u_h^c-u_h^\gamma)\big)_{\mathcal{T}_h} - (f, u_h^c-u_h^\gamma)_{\mathcal{T}_h}\\
&= \big(\overline{\nabla}_{h,g}u, \overline{\nabla}_{h,0}(u_h^c-u_h^\gamma)\big)_{\mathcal{T}_h} - (-\Delta u, u_h^c-u_h^\gamma)_{\mathcal{T}_h}\\
&= \big(\overline{\nabla}_{h,g}u, \overline{\nabla}_{h,0}(u_h^c-u_h^\gamma)\big)_{\mathcal{T}_h} - (\overline{\nabla}_{h,g}u, \overline{\nabla}_{h,0}(u_h^c-u_h^\gamma))_{\mathcal{T}_h}\\
&\quad + \langle\big\{\overline{\nabla}_{h,g}u - \nabla u\big\}\cdot\mathbf{n}, [\![u_h^c-u_h^\gamma]\!]\rangle_{\mathcal{E}_h}\\
&= \langle\big\{\overline{\nabla}_{h,g}u - \nabla u\big\}\cdot\mathbf{n}, [\![u_h^c-u_h^\gamma]\!]\rangle_{\mathcal{E}_h}.
\end{aligned}$$

Applying the Cauchy-Schwarz inequality, the trace theorem with scaling, and Lemma 2.4, we have

$$\begin{aligned}
&B_{h,\gamma}(u-u_h^\gamma, u_h^c-u_h^\gamma)\\
&= \langle\big\{\overline{\nabla}_{h,g}u - \nabla u\big\}\cdot\mathbf{n}, [\![u_h^c-u_h^\gamma]\!]\rangle_{\mathcal{E}_h}\\
&\le \Big(\sum_{e\in\mathcal{E}_h}\|h_e^{1/2}\big\{\overline{\nabla}_{h,g}u - \nabla u\big\}\|_{L^2(e)}^2\Big)^{1/2}\Big(\sum_{e\in\mathcal{E}_h}\|h_e^{-1/2}[\![u_h^c-u_h^\gamma]\!]\|_{L^2(e)}^2\Big)^{1/2}\\
&\le Ch^r\|u\|_{H^{r+1}(\Omega)}\Big(\sum_{e\in\mathcal{E}_h}\|h_e^{-1/2}[\![u_h^c-u_h^\gamma]\!]\|_{L^2(e)}^2\Big)^{1/2}.
\end{aligned} \tag{4.10}$$

Combining (4.7), (4.8), and (4.10), we have

$$\begin{aligned}
&\gamma\sum_{e\in\mathcal{E}_h}\|h_e^{-1/2}[\![u_h^c-u_h^\gamma]\!]\|_{L^2(e)}^2\\
&\le C\big(|\!|\!|u_h^c-u|\!|\!|_{h,1} + Ch^r\|u\|_{H^{r+1}(\Omega)}\big)\Big(\sum_{e\in\mathcal{E}_h}\|h_e^{-1/2}[\![u_h^c-u_h^\gamma]\!]\|_{L^2(e)}^2\Big)^{1/2}.
\end{aligned}$$

Dividing both sides above by $\big(\sum_{e\in\mathcal{E}_h}\|h_e^{-1}[\![u_h^c-u_h^\gamma]\!]\|_{L^2(e)}^2\big)^{1/2}$ and γ gives us

$$\Big(\sum_{e\in\mathcal{E}_h}\|h_e^{-1/2}[\![u_h^c-u_h^\gamma]\!]\|_{L^2(e)}^2\Big)^{1/2} \le \frac{C}{\gamma}\big(|\!|\!|u_h^c-u|\!|\!|_{h,1} + Ch^r\|u\|_{H^{r+1}(\Omega)}\big). \tag{4.11}$$

Lastly, recalling that $u_h^c - u \in H_0^1(\Omega)$, from (2.1) and Lemma 2.4, we have

$$\begin{aligned}
|||u_h^c - u|||_{h,1}^2 &= \frac{1}{2}\|\nabla_{h,0}^+(u_h^c - u)\|_{L^2(\mathcal{T}_h)}^2 + \frac{1}{2}\|\nabla_{h,0}^-(u_h^c - u)\|_{L^2(\mathcal{T}_h)}^2 \\
&\quad + \sum_{e\in\mathcal{E}_h} \|h_e^{-1/2}[\![u_h^c - u]\!]\|_{L^2(e)}^2 \\
&= \frac{1}{2}\|\nabla_{h,0}^+(u_h^c - u)\|_{L^2(\mathcal{T}_h)}^2 + \frac{1}{2}\|\nabla_{h,0}^-(u_h^c - u)\|_{L^2(\mathcal{T}_h)}^2. \qquad (4.12)\\
&\le \frac{1}{2}\|\nabla u_h^c - \nabla u\|_{L^2(\mathcal{T}_h)}^2 + \frac{1}{2}\|\nabla u_h^c - \nabla u\|_{L^2(\mathcal{T}_h)}^2 \\
&= \|\nabla u_h^c - \nabla u\|_{L^2(\Omega)}^2 \\
&\le Ch^{2r}\|u\|_{H^{r+1}(\Omega)}^2
\end{aligned}$$

By combining (4.6), (4.11), and (4.12), we obtain the result

$$\begin{aligned}
|||u_h^c - u_h^\gamma|||_{h,1} &\le \Big(\sum_{e\in\mathcal{E}_h} \|h_e^{-1/2}[\![u_h^c - u_h^\gamma]\!]\|_{L^2(e)}^2\Big)^{1/2} \\
&\le \frac{C}{\gamma}\big(|||u_h^c - u|||_{h,1} + Ch^r\|u\|_{H^{r+1}(\Omega)}\big) \\
&\le \frac{C}{\gamma}\big(Ch^r\|u\|_{H^{r+1}(\Omega)} + Ch^r\|u\|_{H^{r+1}(\Omega)}\big) \\
&= \frac{Ch^r}{\gamma}\|u\|_{H^{r+1}(\Omega)}.
\end{aligned}$$

□

Since $u_h^c, u_h^\gamma \in V_h^r$ and $|||\cdot|||_{h,1}$ is a norm on V_h^r, an immediate consequence of Theorem 4.4 is the following.

Corollary 4.5. *If $u \in H^{r+1}(\Omega)$ for $r \ge 1$ is the solution to (1.1), u_h^γ is the solution to the DWDG method (3.4), and u_h^c is the solution to the CG method (4.1), then*

$$\lim_{\gamma\to\infty} |||u_h^\gamma - u_h^c|||_{h,1} = 0.$$

5. Numerical experiments

In this section, we will verify the results of Theorem 4.4. We will also investigate the effect of the regularity of solutions to (1.2) on the relationship between the penalty parameter γ, the energy error, and the L^2-error of the DWDG approximation.

5.1. **DWDG Converges to CG.** To validate Theorem 4.4, we consider the homogeneous problem

$$\begin{aligned}
-\Delta u &= 2\pi^2 \sin(\pi x)\sin(\pi y) \quad \text{in } \Omega = [0,1]^2, \\
u &= 0 \quad \text{on } \partial\Omega.
\end{aligned} \qquad (5.1)$$

The solution to this equation is $u = \sin(\pi x)\sin(\pi y)$. The approximations and error calculations were done on a fixed mesh with $h = \frac{1}{32}$ for linear basis polynomials and $h = \frac{1}{16}$ for quadratic and cubic basis polynomials. Based on the proof of Theorem 4.4 and [16, Lemma IV.4], we measured the error in

- the energy norm $|||u_h^c - u_h^\gamma|||_{h,1}$,
- the H^1 semi-norm $\|\nabla(u_h^c - u_h^\gamma)\|_{L^2(\mathcal{T}_h)}$,

- the jump error $\left(\sum_{e\in\mathcal{E}_h}\|h_e^{-1/2}[\![u_h^c-u_h^\gamma]\!]\|^2_{L^2(e)}\right)^{1/2}$.

The error and rates using linear, quadratic, and cubic basis polynomials for the DWDG approximation with varying values of the penalty parameter γ can be found in Table 1. In all three error measurements, we are able to achieve a rate of 1 with respect to γ as $\gamma\to\infty$. Note that the matrix corresponding to the bilinear form $B_{h,\gamma}(\cdot,\cdot)$ will require special treatment for larger values of γ due to the spectral radius increasing instep with the value of γ.

TABLE 1. Energy error, H^1 semi-norm error, jump error and their respective rates for (5.1).

Poly	γ	$\|\|\|u_h^c-u_h^\gamma\|\|\|_{h,1}$	Rate	$\|\nabla(u_h^c-u_h^\gamma)\|_{L^2(\mathcal{T}_h)}$	Rate	Jump Error	Rate
$r=1$	1	1.3514e-02	—	1.1934e-02	—	9.4287e-03	—
	10	7.2250e-03	0.2719	6.3040e-03	0.2772	4.9789e-03	0.2773
	10^2	1.2874e-03	0.7491	1.1171e-03	0.7515	8.8320e-04	0.7511
	10^3	1.3971e-04	0.9645	1.2114e-04	0.9648	9.5790e-05	0.9647
	10^4	1.4094e-05	0.9962	1.2237e-05	0.9956	9.6608e-06	0.9963
	10^5	1.4440e-06	0.9895	1.4043e-06	0.9402	9.6691e-07	0.9996
$r=2$	1	1.0215e-03	—	9.9343e-04	—	5.4330e-04	—
	10	6.9298e-04	0.1685	7.2228e-04	0.1384	3.4854e-04	0.1928
	10^2	1.7932e-04	0.5871	2.0400e-04	0.5491	8.4431e-05	0.6157
	10^3	2.1642e-05	0.9183	2.5125e-05	0.9095	1.0034e-05	0.9250
	10^4	2.2109e-06	0.9907	2.5726e-06	0.9897	1.0232e-06	0.9915
	10^5	2.2157e-07	0.9991	2.5771e-07	0.9992	1.0253e-07	0.9991
$r=3$	1	1.0741e-05	—	1.4247e-05	—	4.9554e-06	—
	10	7.7927e-06	0.1393	1.0155e-05	0.1470	3.5359e-06	0.1466
	10^2	2.1274e-06	0.5638	2.7326e-06	0.5701	9.4950e-07	0.5710
	10^3	2.5835e-07	0.9156	3.3106e-07	0.9167	1.1482e-07	0.9175
	10^4	2.6405e-08	0.9905	3.3830e-08	0.9906	1.1730e-08	0.9907
	10^5	2.6645e-09	0.9961	3.4807e-09	0.9876	1.1755e-09	0.9991

5.2. **Relationship between γ and the L^2-error.** For our experiments, we will test the DWDG methods for approximating (1.2). We will find the L^2-error on a fixed mesh with $h=\frac{1}{16}$. We will run the DWDG approximation with two sets of γ's to get an idea of the behavior of the L^2-error near $\gamma=0$ as well as for large values of γ. To determine the behavior of the L^2-error around $\gamma=0$ we chose $\gamma\in\{-2,-1.8,-1.6,-1.4,-1.2,\cdots,10\}$. Since the constant C_* has a complex derivation, the exact value is generally unknown. Going only as low as $\gamma=-2$ should guarantee that the method is stable, and it gives us more information about the effect of γ decreasing towards zero and becoming negative. To determine the behavior of the L^2-error as $\gamma\to\infty$ we chose $\gamma\in\{10,10^{1.5},10^2,10^{2.5},10^3,10^{3.5},10^4,10^{4.5},10^5\}$ to reflect the results found in Table 1. We measure the error of the DWDG approximation in the the L^2 norm $\|u-u_h^\gamma\|_{L^2(\mathcal{T}_h)}$. Since the choice of starting mesh, based on minimal angle, did not have a noticeable effect on the L^2-error of the DWDG approximation [16], we have chosen to preform our experiments on a uniform criss-cross mesh. LDG methods are known to require $\gamma>0$ for cris-cross meshes [13]. Thus, the choice represents a potentially challenging meshing strategy for DWDG methods without penalization.

The numerical experiment was run on the problem

$$\begin{aligned} -\Delta u_\alpha &= f \quad \text{in } \Omega=[-1,1]^2,\\ u_\alpha|_{\partial\Omega} &= g \quad \text{on } \partial\Omega, \end{aligned} \tag{5.2}$$

where $\alpha > 0$ is a constant. The functions f and g are chosen so that the solution for (5.2) is

$$u_\alpha(x,y) = \begin{cases} \cos(\frac{\pi}{2}y) & \text{if } x < 0, \\ \cos(\frac{\pi}{2}y) + x^\alpha & \text{if } x \geq 0. \end{cases}$$

This solution belongs to $H^{\alpha+\frac{1}{2}}(\Omega)$ but does not belong to $H^{\alpha+1/2+\epsilon}(\Omega)$ for all $\epsilon > 0$ [7]. To test the impact of the regularity of the solution on the choice of γ we will choose $\alpha \in \{1.5, 2.5, 3.5, 4.5\}$. We have also plotted the CG approximation L^2-error in each plot of Figure 1. Note that the CG L^2-error was larger than the DWDG L^2-errors in Figure 2, even though the CG L^2-error was not plotted. The CG L^2-error values are given instead of plotted for each combination of α and the smaller γ in Figure 2, as the relatively large difference in the L^2-error for the DWDG and CG method prevented both errors to be plotted while visually retaining the shape of the DWDG's L^2-error curve.

For the linear DWDG methods, we see a check-mark relationship between γ and the L^2-error of the approximation when γ is close to zero (see Figure 2). When the solution $u \in H^2(\Omega)$, we see an upward trend in the L^2-error after $\gamma = 5$ creating a wide check-mark relationship. As the regularity of the solution increased, we see the bottom of the check-mark relationship move to the left, indicating that if the regularity was high enough, we would see a strictly increasing relationship between γ and the DWDG L^2-error. This is a similar observation for the linear DWDG approximation in [16], where refining the mesh also moved the bottom of the check-mark relationship to the left. For the larger values of γ (see Figure 1), we see a strictly increasing relationship that tapers off as the DWDG L^2-error approaches the CG L^2-error. From this, we conjecture that there is a strictly increasing relationship between the L^2-error and γ for the linear DWDG approximation for values of γ that are large enough or if the regularity of the solution is high enough.

For the DWDG methods with quadratic and cubic basis polynomials, we see a strictly increasing relationship between γ and the L^2-error of the DWDG approximation when looking at the smaller range of γ (see Figure 2). For the larger range of γ (see Figure 1) a strictly increasing relationship was persistent for quadratic basis functions. For cubic basis functions, we see a strictly increasing trend until the largest values of γ when $u \in H^3(\Omega)$ or $u \in H^4(\Omega)$.

Overall, we observe that as the regularity of the solution to (1.1) increased, we could see a strictly increasing trend between the L^2-error and γ for $\gamma \geq 0$. It is of interest to note that as $\gamma \to \infty$, the spectral radius of the DWDG matrix from the bilinear form $B_{h,\gamma}(\cdot,\cdot)$ will scale with the choice of γ. Though we choose large values of γ to show the convergence of the DWDG approximation to the CG approximation in our numerical results, the DWDG approximation always had lower errors than the CG approximation. Furthermore, the best L^2-errors were found near $\gamma = 0$. The choice of $\gamma = 0$ simplifies the approximation, and it appears to yield a more accurate approximation.

Acknowledgements. This work was supported by the National Science Foundation under Grant DMS-2111059. Y. Zhang was supported by the National Science Foundation under Grant DMS-2111004.

References

[1] R. A. Adams, J. JF. Fournier; *Sobolev spaces*, Elsevier, 2003.

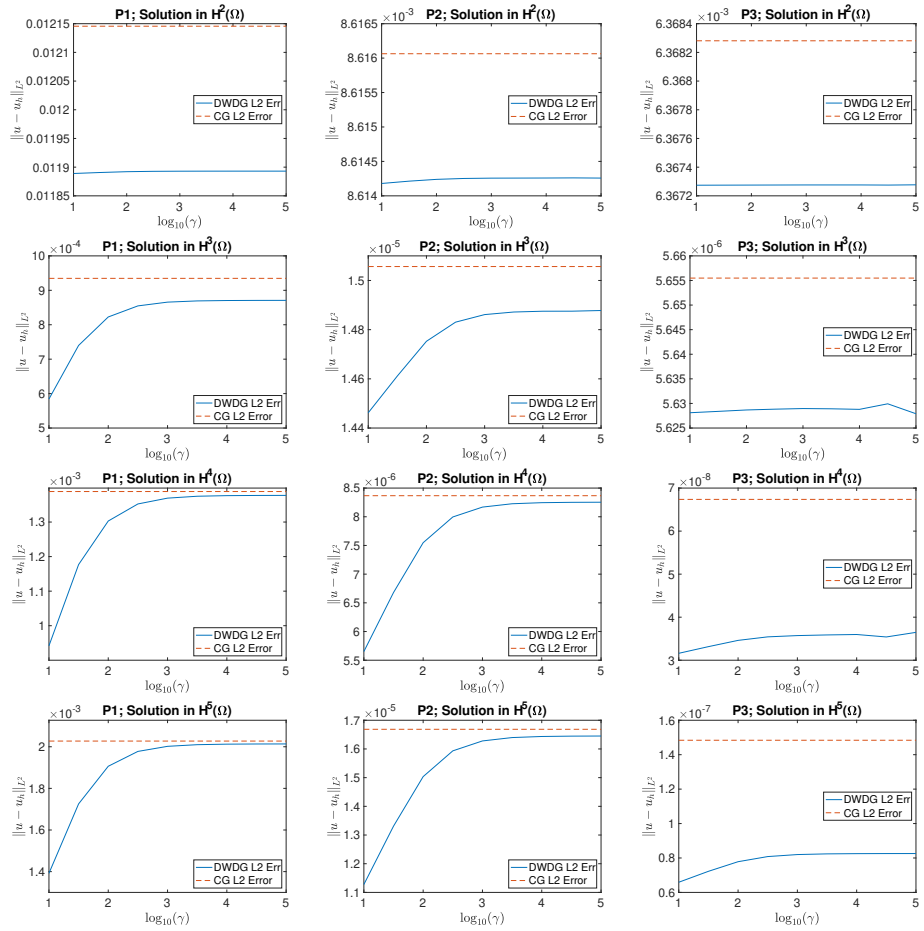

FIGURE 1. DWDG L^2-error vs large γ plots for linear (left column), quadratic (middle column) and cubic (right column) basis polynomials on a uniform mesh with $h = 1/16$.

[2] D. Arnold, F. Brezzi, B. Cockburn, L. Marini; *Unified analysis of discontinuous Galerkin methods for elliptic problems*, SINUM **39** (2002), no. 5, 1749–1779.

[3] S. Brenner, R. Scott; *The mathematical theory of finite element methods*, vol. 15, Springer Science & Business Media, 2007.

[4] S. C. Brenner; *Poincaré–Friedrichs inequalities for piecewise H^1 functions*, SIAM J Numer Anal **41** (2003), no. 1, 306–19.

[5] E. Burman, A. Quarteroni, B. Stamm; *Interior penalty continuous and discontinuous finite element approximations of hyperbolic equations*, J Sci Comput **43** (2010), no. 3, 293–312.

[6] A. Cangiani, J. Chapman, E. Georgoulis, M. Jensen; *On local super-penalization of interior penalty discontinuous galerkin methods*, International Journal of Numerical Analysis and Modeling **11** (2013), 478–495.

[7] Paul Castillo, Bernardo Cockburn, Ilaria Perugia, Dominik Schötzau; *An a priori error analysis of the local discontinuous galerkin method for elliptic problems*, SIAM Journal on Numerical Analysis **38** (2000), no. 5, 1676–1706.

[8] P. Ciarlet; *The finite element method for elliptic problems*, Classics in applied mathematics, no. 40, SIAM, Philadelphia, PA, 2002.

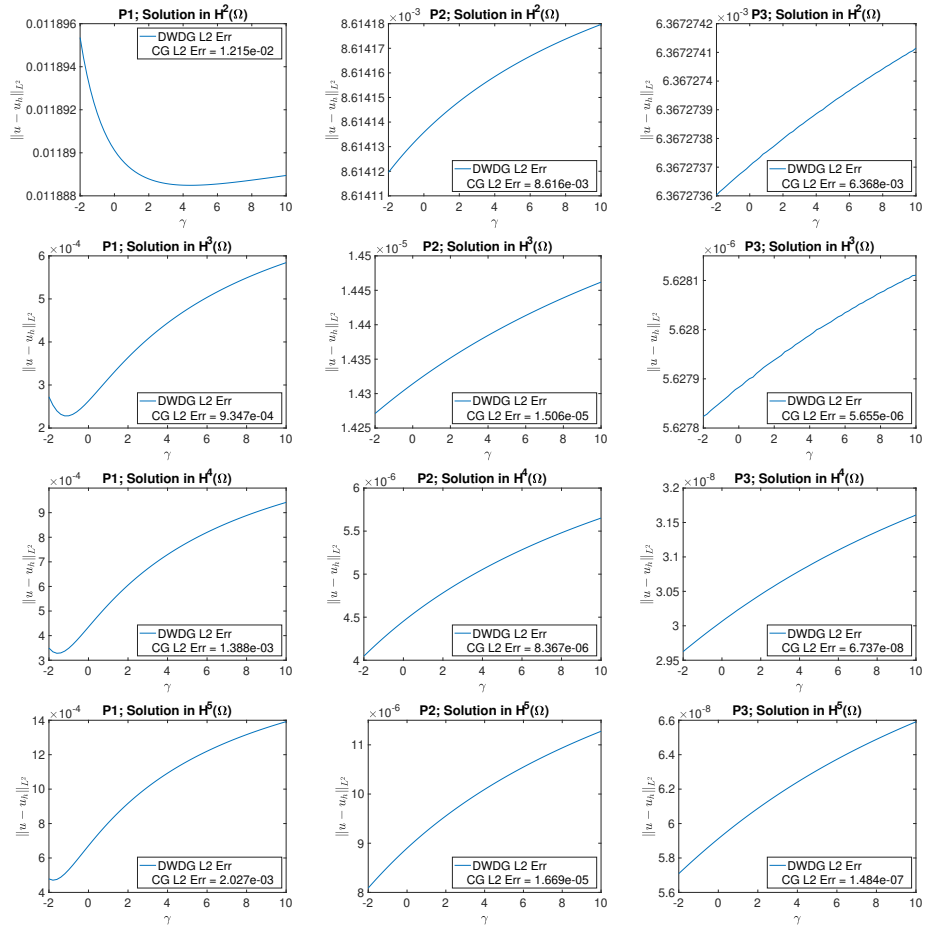

FIGURE 2. DWDG L^2-error vs small γ plots for linear (left column), quadratic (middle column) and cubic (right column) basis polynomials on a uniform mesh with $h = 1/16$.

[9] B. Cockburn, B. Dong; *An analysis of the minimal dissipation local discontinuous Galerkin method for convection-diffusion problems*, J Sci Comput **32** (2007), no. 2, 233–262.

[10] W. Feng, T. L. Lewis, S. M. Wise; *Discontinuous Galerkin derivative operators with applications to second-order elliptic problems and stability*, Math Meth Appl Sci **38** (2015), no. 18, 5160–5182.

[11] X. Feng, T. Lewis, M. Neilan; *Discontinuous Galerkin finite element differential calculus and applications to numerical solutions of linear and nonlinear partial differential equations*, J Comput Appl Math **299** (2016), 68–91.

[12] M. Larson, A. Niklasson; *Conservation properties for the continuous and discontinuous Galerkin methods*, Chalmers Finite Element Center Preprint **8**, 2000.

[13] T. Lewis; *Distributional derivatives and stability of discontinuous Galerkin finite element approximation methods*, Electron J Differ Eq (2016), 59–76.

[14] T. Lewis M. Neilan; *Convergence analysis of a symmetric dual-wind discontinuous Galerkin method: Convergence analysis of DWDG*, J Sci Comput **59** (2014), no. 3, 602–625.

[15] T. Lewis, A. Rapp, Y. Zhang; *Convergence analysis of symmetric dual-wind discontinuous galerkin approximation methods for the obstacle problem*, J Math Anal Appl (2020), 123840.

[16] A. Rapp; *Symmetric dual-wind discontinuous Galerkin methods for elliptic variational inequalities*, Ph.D. thesis, The University of North Carolina at Greensboro, 2020.

Thomas Lewis
Department of Mathematics and Statistics, The University of North Carolina at Greensboro, Greensboro, NC 27402, USA
Email address: tllewis3@uncg.edu

Aaron Rapp
Department of Mathematical Sciences, The University of the Virgin Islands, Charlotte Amalie West, St. Thomas, 00820, United States Virgin Islands
Email address: aaron.rapp@uvi.edu

Yi Zhang
Department of Mathematics and Statistics, The University of North Carolina at Greensboro, Greensboro, NC 27402, USA
Email address: y_zhang7@uncg.edu